# Measurement of the $\Omega_c^0$ lifetime at Belle II

F. Abudinén, I. Adachi, L. Aggarwal, H. Ahmed, H. Aihara, N. Akopov, A. Aloisio, N. Anh Ky, T. Aushev, V. Aushev, H. Bae, P. Bambade, Sw. Banerjee, J. Baudot, M. Bauer, A. Beaubien, J. Becker, P. K. Behera, J. V. Bennett, E. Bernieri, F. U. Bernlochner, V. Bertacchi, M. Bertemes, E. Bertholet, M. Bessner, S. Bettarini, B. Bhuyan, F. Bianchi, T. Bilka, D. Biswas, D. Bodrov, A. Bolz, J. Borah, A. Bozek, M. Bračko, P. Branchini, R. A. Briere, T. E. Browder, A. Budano, S. Bussino, M. Campajola, L. Cao, G. Casarosa, C. Cecchi, M.-C. Chang, P. Cheema, V. Chekelian, Y. Q. Chen, K. Chilikin, K. Chirapatpimol, H.-E. Cho, K. Cho, S.-J. Cho, S.-K. Choi, S. Choudhury, D. Cinabro, L. Corona, S. Cunliffe, S. Das, F. Dattola, E. De La Cruz-Burelo, S. A. De La Motte, G. de Marino, G. De Nardo, M. De Nuccio, G. De Pietro, R. de Sangro, M. Destefanis, S. Dey, A. De Yta-Hernandez, R. Dhamija, A. Di Canto, F. Di Capua, J. Dingfelder, Z. Doležal, I. Domínguez Jiménez, T. V. Dong, M. Dorigo, K. Dort, S. Dreyer, S. Dubey, G. Dujany, P. Ecker, M. Eliachevitch, D. Epifanov, P. Feichtinger, T. Ferber, D. Ferlewicz, T. Fillinger, G. Finocchiaro, A. Fodor, F. Forti, B. G. Fulsom, E. Ganiev, V. Gaur, A. Gaz, A. Gellrich, G. Ghevondyan, R. Giordano, A. Giri, A. Glazov, B. Gobbo, R. Godang, P. Goldenzweig, W. Gradl, S. Granderath, E. Graziani, D. Greenwald, T. Gu, Y. Guan, K. Gudkova, J. Guilliams, K. Hayasaka, H. Hayashii, S. Hazra, C. Hearty, I. Heredia de la Cruz, M. Hernández Villanueva, A. Hershenhorn, T. Higuchi, E. C. Hill, H. Hirata, M. Hohmann, C.-L. Hsu, T. Iijima, K. Inami, G. Inguglia, N. Ipsita, A. Ishikawa, S. Ito, R. Itoh, M. Iwasaki, P. Jackson, W. W. Jacobs, D. E. Jaffe, E.-J. Jang, S. Jia, Y. Jin, K. K. Joo, H. Junkerkalefeld, A. B. Kaliyar, K. H. Kang, R. Karl, G. Karyan, C. Kiesling, C.-H. Kim, D. Y. Kim, K.-H. Kim, Y.-K. Kim, H. Kindo, K. Kinoshita, P. Kodyš, T. Koga, S. Kohani, K. Kojima, T. Konno, A. Korobov, S. Korpar, E. Kovalenko, R. Kowalewski, T. M. G. Kraetzschmar, P. Križan, P. Krokovny, J. Kumar, K. Kumara, T. Kunigo, A. Kuzmin, Y.-J. Kwon, S. Lacaprara, T. Lam, L. Lanceri, J. S. Lange, M. Laurenza, K. Lautenbach, R. Leboucher, C. Li, L. K. Li, J. Libby, K. Lieret, Z. Liptak, Q. Y. Liu, D. Liventsev, S. Longo, A. Lozar, T. Lueck, C. Lyu, M. Maggiora, R. Maiti, R. Manfredi, E. Manoni, S. Marcello, C. Marinas, A. Martini, T. Martinov, L. Massaccesi, M. Masuda, S. K. Maurya, J. A. McKenna, F. Meier, M. Merola, F. Metzner, M. Milesi, C. Miller, K. Miyabayashi, R. Mizuk, N. Molina-Gonzalez, S. Moneta, H.-G. Moser, M. Mrvar, R. Mussa, I. Nakamura, M. Nakao, H. Nakayama, Y. Nakazawa, A. Narimani Charan, M. Naruki, Z. Natkaniec, A. Natochii, L. Nayak, M. Nayak, G. Nazaryan, N. K. Nisar, S. Ogawa, H. Ono, Y. Onuki, E. R. Oxford, A. Paladino, A. Panta, E. Paoloni, S. Pardi, H. Park, S.-H. Park, A. Passeri, S. Paul, T. K. Pedlar, I. Peruzzi, R. Peschke, R. Pestotnik, M. Piccolo, L. E. Piilonen, P. L. M. Podesta-Lerma, T. Podobnik, S. Pokharel, L. Polat, C. Praz, S. Prell, E. Prencipe, M. T. Prim, H. Purwar, N. Rad, P. Rados, S. Raiz, A. Ramirez Morales, M. Reif, S. Reiter, M. Remnev, I. Ripp-Baudot, G. Rizzo, S. H. Robertson, J. M. Roney, A. Rostomyan, N. Rout, G. Russo, D. A. Sanders, S. Sandilya, A. Sangal, Y. Sato, V. Savinov, B. Scavino, J. Schueler, C. Schwanda, A. J. Schwartz, B. Schwenker, Y. Seino, A. Selce, K. Senyo, J. Serrano, M. E. Sevior, C. Sfienti, C. P. Shen, X. D. Shi, T. Shillington, A. Sibidanov, J. B. Singh, J. Skorupa, R. J. Sobie, A. Soffer, E. Solovieva, S. Spataro, B. Spruck, M. Starič, S. Stefkova, Z. S. Stottler, R. Stroili, J. Strube, M. Sumihama, K. Sumisawa, W. Sutcliffe, S. Y. Suzuki, H. Svidras, M. Takizawa, U. Tamponi, K. Tanida, H. Tanigawa, F. Tenchini, A. Thaller, R. Tiwary, D. Tonelli, E. Torassa, N. Toutounji, K. Trabelsi, M. Uchida, I. Ueda, Y. Uematsu, T. Uglov, K. Unger, Y. Unno, K. Uno, S. Uno, Y. Ushiroda, S. E. Vahsen, R. van Tonder, G. S. Varner, K. E. Varvell, A. Vinokurova, L. Vitale, V. Vobbilisetti, H. M. Wakeling, E. Wang, M.-Z. Wang, X. L. Wang, A. Warburton, M. Watanabe, S. Watanuki, M. Welsch, C. Wessel, E. Won, B. D. Yabsley, S. Yamada, W. Yan, S. B. Yang, H. Ye, J. Yelton, J. H. Yin, Y. M. Yook, K. Yoshihara, C. Z. Yuan, L. Zani, Y. Zhang, V. Zhilich, Q. D. Zhou, X. Y. Zhou, V. I. Zhukova, and R. Žlebčík

(The Belle II Collaboration)

We report on a measurement of the $\Omega_c^0$ lifetime using $\Omega_c^0 \to \Omega^-\pi^+$ decays reconstructed in $e^+e^- \to c\overline{c}$ data collected by the Belle II experiment and corresponding to $207\,\mathrm{fb}^{-1}$ of integrated luminosity. The result, $\tau(\Omega_c^0) = 243 \pm 48\,(\mathrm{stat}) \pm 11\,(\mathrm{syst})\,\mathrm{fs}$, agrees with recent measurements indicating that the $\Omega_c^0$ is not the shortest-lived weakly decaying charmed baryon.

The lifetime hierarchy of beauty hadrons is accurately predicted using the so-called heavy-quark expansion, which expresses the decay rate of heavy hadrons as an expansion in inverse powers of the heavy-quark mass $m_b$ [1–6]. An accurate prediction of the hierarchy of charmed hadrons is more challenging because higher-order terms in $1/m_c$ and contributions from spectator quarks cannot be neglected and result in larger uncertainties. While the lifetimes of charmed mesons are known to high precision, the lifetimes of charmed baryons are

less well measured [7].

Since its lifetime was first measured in 1995 [8, 9], the $\Omega_c^0$ baryon was believed to be the shortest lived among the four singly charmed baryons that decay weakly [10], in agreement with theoretical expectations [11, 12]. In 2018, using $\Omega_c^0 \to pK^-K^-\pi^+$ decays originating from semileptonic $b$-hadron decays, the LHCb collaboration measured the $\Omega_c^0$ lifetime to be $268 \pm 24 \pm 10 \pm 2$ fs, where the uncertainties are statistical, systematic, and from the $D^+$ lifetime used as normalization [13]. This value is nearly four times larger than, and inconsistent with, the previous world average of $69 \pm 12$ fs [10], resulting in the new hierarchy $\tau(\Xi_c^0) < \tau(\Lambda_c^+) < \tau(\Omega_c^0) < \tau(\Xi_c^+)$. Another recent measurement from LHCb using promptly produced $\Omega_c^0 \to pK^-K^-\pi^+$ decays confirms their previous result with better precision, $276.5 \pm 13.4 \pm 4.4 \pm 0.7$ fs, where the last uncertainty is from the $D^0$ lifetime used as normalization [14]. No experimental confirmation of the LHCb results exists. Why the heavy-quark expansion failed to predict the newly observed hierarchy is being debated [15, 16].

In this Letter, we report on a measurement of the $\Omega_c^0$ lifetime using $\Omega_c^0 \to \Omega^-\,\pi^+$ decays reconstructed in $e^+e^- \to c\bar{c}$ events at Belle II. Charge-conjugated decays are included throughout this Letter. The $e^+e^-$ collision data used are collected at center-of-mass energies at or near the $\Upsilon(4S)$ mass and correspond to an integrated luminosity of $207\,\text{fb}^{-1}$. Assuming a lifetime consistent with the LHCb measurement, $\Omega_c^0$ baryons produced in $e^+e^- \to c\bar{c}$ events at Belle II have a Lorentz boost that, on average, displaces their decay vertices by 100 μm from the $e^+e^-$ interaction point (IP), where they are produced. The decay time is measured from the projection of the displacement $\vec{L}$ along the direction of the momentum $\vec{p}$, as $t = m\vec{L} \cdot \vec{p}/|\vec{p}|^2$, where $m$ is the known mass of the $\Omega_c^0$ baryon [7]. The decay-time uncertainty $\sigma_t$ is calculated by propagating the uncertainties in $\vec{L}$ and $\vec{p}$, including their correlations. The lifetime is determined using a fit to the $(t, \sigma_t)$ distributions of the reconstructed $\Omega_c^0$ candidates. To minimize bias, an arbitrary and unknown lifetime offset is applied to the data. The offset is revealed only after we finalized the entire analysis procedure and determined all uncertainties.

The Belle II detector [17] is built around the collision point of the SuperKEKB asymmetric-energy $e^+e^-$ collider [18] and consists of subsystems arranged in a cylindrical geometry around the beam pipe. The innermost is a tracking subsystem consisting of a two-layer silicon-pixel detector (PXD) surrounded by a four-layer double-sided silicon-strip detector (SVD) and a 56-layer central drift chamber (CDC). Only 15% of the azimuthal angle is covered by the second PXD layer for the collection of these data. A time-of-propagation counter in the barrel and an aerogel ring-imaging Cherenkov detector in the forward end cap provide information used for the identification of charged particles. An electromagnetic calorimeter consisting of CsI(Tl) crystals fills the remaining volume inside a 1.5 T superconducting solenoid and provides energy and timing measurements for photons and electrons. A $K_L^0$ and muon detection subsystem is installed in the iron flux return of the solenoid. The $z$ axis of the laboratory frame is defined as the central axis of the solenoid, with its positive direction defined as the direction opposite the positron beam.

Events are reconstructed using the Belle II software framework [19, 20] using selection requirements that ensure large signal efficiency and avoid biases on decay time or variation of the signal efficiency as a function of decay time, as verified in simulation. The simulation uses KKMC [21] to generate quark-antiquark pairs from $e^+e^-$ collisions, PYTHIA8 [22] to simulate the quark hadronization, EVTGEN [23] to decay the hadrons, and GEANT4 [24] to simulate the detector response.

Events enriched in signal $\Omega_c^0 \to \Omega^-\pi^+$ decays, with $\Omega^- \to \Lambda^0(\to p\pi^-)K^-$, are selected by rejecting events consistent with Bhabha scattering and by requiring at least three charged particles, with transverse momenta greater than 200 MeV/$c$, that are consistent with originating from the $e^+e^-$ interaction. These charged particles are not required to belong to the $\Omega_c^0 \to \Omega^-\pi^+$ decay. Candidate $\Lambda^0 \to p\pi^-$ decays are formed using pairs of oppositely charged particles, one of which must be identified as a proton. The decay vertex of the $\Lambda^0$ candidate is required to be more than 0.35 cm away from the IP. The $\Lambda^0$ candidates are combined with negatively charged kaon candidates having transverse momenta greater than 0.15 GeV/$c$ to form $\Omega^- \to \Lambda^0 K^-$ decays. The $\Omega^-$ decay vertex must lie between the $\Lambda^0$ vertex and the IP and be at least 0.5 mm from the IP. For both the $\Lambda^0$ and the $\Omega^-$ candidates, the angle between its momentum and its displacement from the IP must be smaller than 90°. Candidate $\Omega_c^0 \to \Omega^-\pi^+$ decays are formed by combining the selected $\Omega^-$ candidates with positively charged particles that are consistent with originating from the $e^+e^-$ interaction and have momenta greater than 0.5 GeV/$c$. To reduce combinatorial background and $\Omega_c^0$ candidates originating from $B$ decays, we require the scaled momentum of the $\Omega_c^0$ candidate be larger than 0.6. The scaled momentum is $p_{\text{cms}}/\sqrt{s/4 - m(\Omega^-\pi^+)^2}$, where $p_{\text{cms}}$ is the momentum of the $\Omega_c^0$ candidate in the $e^+e^-$ center-of-mass system, $s$ is the squared center-of-mass energy, and $m(\Omega^-\pi^+)$ is the reconstructed $\Omega_c^0$ mass. A decay-chain vertex fit constrains the tracks according to the decay topology and constrains the $\Omega_c^0$ candidate to originate from the $e^+e^-$ interaction region [25]. The interaction region has typical dimensions of 250 μm along the $z$ axis and of 10 μm and 0.3 μm in the two directions transverse to the $z$ axis. Its position and size vary over time and are measured using $e^+e^- \to \mu^+\mu^-$ events. Only candidates with fit probabilities larger than 0.001 and with $\sigma_t$ values smaller than 1.0 ps are retained for further analysis. The vertex fit updates the track parameters of the final-state particles, and the updated parameters are used in the subsequent analysis. The $\Lambda^0$ and $\Omega^-$ candidates are required to have masses within approximately three units of mass resolution (or standard deviations) of their known

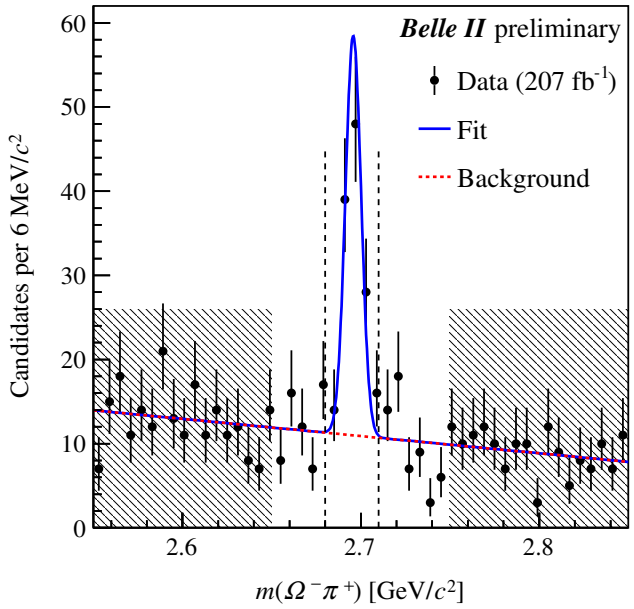


Figure 1: Mass distribution for $\Omega_c^0 \to \Omega^-\pi^+$ candidates with fit projections overlaid. The vertical dashed lines enclose the signal region; the shaded area indicates the sideband.

values [7]. The mass of the $\Omega_c^0$ candidate must be in the range $[2.55, 2.85]\,\mathrm{GeV}/c^2$. After these requirements, about 0.5% of events have multiple $\Omega_c^0$ candidates; for these events, the candidate with the highest vertex-fit probability is retained. An unbinned maximum likelihood fit to the $m(\Omega^-\pi^+)$ distribution is used to determine the signal purity in the signal region defined by $2.68 < m(\Omega^-\pi^+) < 2.71\,\mathrm{GeV}/c^2$ (Fig. 1). In the fit, the $\Omega_c^0$ signal is modeled with a Gaussian distribution, and the background is modeled with a straight line. The signal region contains approximately 132 candidates with a signal purity of $(66.5 \pm 3.3)\%$.

The lifetime is determined using a maximum-likelihood fit to the unbinned $(t, \sigma_t)$ distribution of the candidates populating the signal region. The signal probability-density function (PDF) is the convolution of an exponential distribution in $t$ with a Gaussian resolution function that depends on $\sigma_t$, multiplied by the PDF of $\sigma_t$. The resolution function's mean is a free parameter of the fit to account for a possible bias in the determination of the decay time; its width is the per-candidate $\sigma_t$ scaled by a free parameter $s$ to account for a possible misestimation of the decay-time uncertainty. The background in the signal region is empirically modeled from data with $m(\Omega^-\pi^+)$ in the *sideband* $[2.55, 2.65]\cup[2.75, 2.85]\,\mathrm{GeV}/c^2$ (Fig. 1). The sideband is taken to contain exclusively background candidates and be representative of the background in the signal region, as verified in simulation. The background PDF is the sum of a $\delta$ function at zero and an exponential component, both convolved with a Gaussian resolution function having a free mean and a width corresponding to $\sigma_t$ scaled by a free parameter. To better constrain the background parameters, a simultaneous fit to the candidates in the signal region and the sideband is performed. The background fraction is Gaussian-constrained to the value measured in the $m(\Omega^-\pi^+)$ fit. The PDFs of $\sigma_t$ are histogram templates derived directly from the data. The signal template is derived from the candidates in the signal region after subtracting the scaled distribution of the sideband data. The background template is obtained directly from the sideband data. No direct input from simulation is used in the fit.

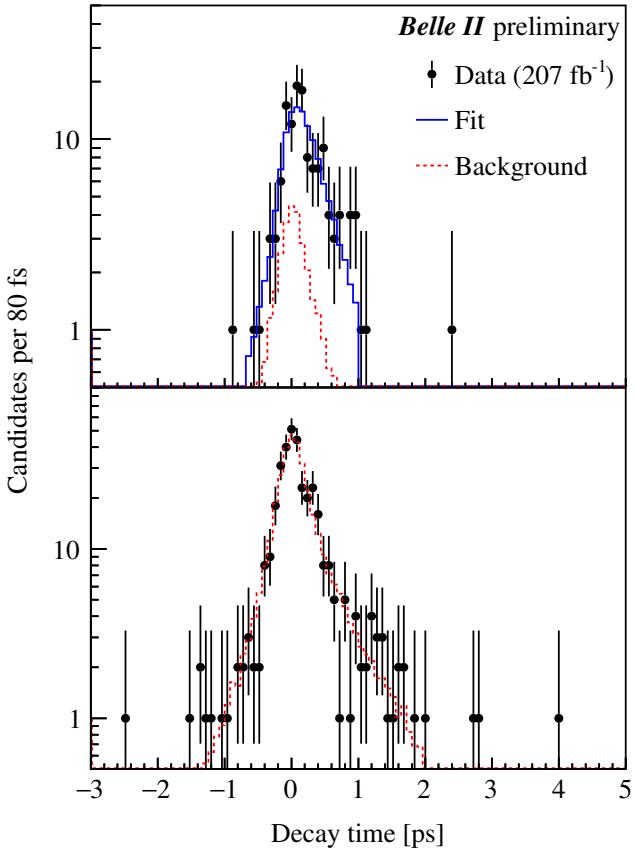


Figure 2: Decay-time distributions for $\Omega_c^0 \to \Omega^-\pi^+$ candidates populating (top) the signal region and (bottom) the sideband with fit projections overlaid.

The distributions of decay time and decay-time uncertainty are shown in Figs. 2 and 3 with fit projections overlaid. The $\Omega_c^0$ lifetime is measured to be $243 \pm 48\,\mathrm{fs}$, the mean of the signal resolution function is $-18 \pm 41\,\mathrm{fs}$, and the scaling factor of the width is $1.35 \pm 0.20$, where the uncertainties are statistical only.

The following sources of systematic uncertainties are considered: fit bias, resolution model, treatment of background contamination, imperfect alignment of the tracking detectors, and uncertainties in the momentum scale and in the input $\Omega_c^0$ mass. Table I lists all contributions and their total, calculated as the sum in quadrature of the individual contributions.

The lifetime fit is tested on data generated by ran-

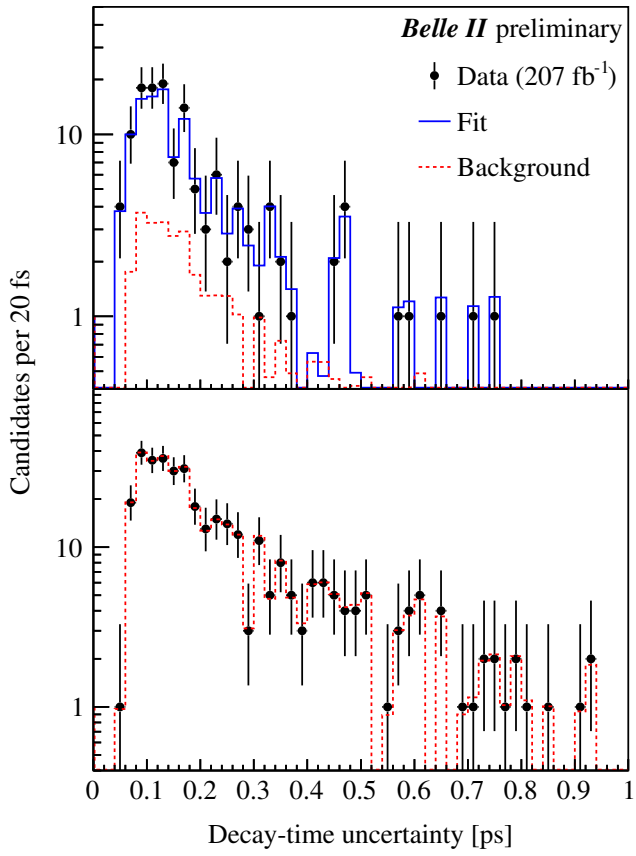


Figure 3: Decay-time-uncertainty distributions for $\Omega_c^0 \to \Omega^-\pi^+$ candidates populating (top) the signal region and (bottom) the sideband with fit projections overlaid.

Table I: Systematic uncertainties.

| Source | Uncertainty (fs) |
|---|---|
| Fit bias | 3.4 |
| Resolution model | 6.2 |
| Background model | 8.3 |
| Detector alignment | 1.6 |
| Momentum scale | 0.2 |
| Input $\Omega_c^0$ mass | 0.2 |
| Total | 11.0 |

domly sampling the fit PDF with parameters fixed to the values found in the fit to the data and with lifetime values varied between 60 fs and 300 fs. One thousand pseudoexperiments, each the same size as the data, are generated for each tested lifetime value. A $-3.4$ fs bias is observed for lifetime values close to the fit result of 243 fs. Its absolute value is assigned as a symmetric systematic uncertainty.

Simulation shows that the resolution function has tails that are inconsistent with a Gaussian model. The effect on the measured lifetime due to using our imperfect resolution model is quantified using one thousand samples of signal-only simulated decays, each the same size as the data. The samples are obtained by resampling, with replacement, from a sample of simulated $e^+e^-$ collisions corresponding to five times the data size. For each sample the fit is performed and the measured lifetime is compared to the true lifetime of the parent simulation sample. The average difference between measured and true lifetimes, 2.8 fs, is corrected for the known fit bias of $-3.4$ fs and the resulting value, 6.2 fs, is assigned as a systematic uncertainty due to the imperfect resolution model.

For signal decays, the decay-time resolution function has a mean that depends nearly linearly on the candidate mass, and is expected to average out for a symmetric range of candidate masses. We check that the associated uncertainty in the measured lifetime is negligible by varying the boundaries of the signal region.

In simulation, the $(t, \sigma_t)$ distribution of the candidates in the sideband describes the background candidates in the signal region well. The same might not hold for the data and this could bias the result. To quantify this bias, we generate and fit to one thousand pseudoexperiments, each the same size and with the same signal-to-background proportion as that of the data. In the generation, signal and background candidates populating the signal region are sampled from the fit PDFs, using input parameters equal to those determined from the fit to the data. Generated background candidates in the signal region thus feature the same $(t, \sigma_t)$ distribution as the data. In contrast, candidates in the sideband are sampled from simulated $e^+e^-$ collisions. In this manner, the pseudoexperiments feature sideband data that differ from the background in the signal region with the same level of disagreement as observed between data and simulation. The averaged difference between the measured and generated lifetimes, corrected for the previously estimated biases due to the fit and to the resolution model, is $6.2 \pm 1.9$ fs. Various definitions of the sideband are tried: $[2.55, 2.64] \cup [2.76, 2.85]\,\text{GeV}/c^2$, $[2.55, 2.66] \cup [2.74, 2.85]\,\text{GeV}/c^2$, $[2.55, 2.65]\,\text{GeV}/c^2$, and $[2.75, 2.85]\,\text{GeV}/c^2$. The latter region shows a significant deviation in fitted lifetime from the nominal result. The deviation, 8.3 fs, is consistent with the pseudoexperiments study and is assigned as a systematic uncertainty due to the modeling of the background $(t, \sigma_t)$ distribution.

In the lifetime fit, the fraction of background candidates in the signal region is constrained by the result of the fit to the $m(\Omega^-\pi^+)$ distribution. When we change this background fraction to values obtained from fitting to the $m(\Omega^-\pi^+)$ distribution with alternative signal and background PDFs, the change in the measured lifetime is negligible.

In Belle II, track parameters are periodically calibrated to correct for misalignment and deformation of internal components of the PXD and SVD, and for the relative alignments of the PXD, SVD, and CDC. Misalignment can bias the measurement of the decay lengths and hence of the decay times. To quantify the effect of possible

residual misalignment on the measured lifetime, large samples of signal decays are simulated with various misalignment configurations. Lifetime residuals with respect to perfectly aligned simulation are estimated, and their root mean square, 1.6 fs, is assigned as a systematic uncertainty due to possible detector misalignment.

Uncertainties in the knowledge of the absolute momentum scale and in the world-average value of the $\Omega_c^0$ mass [7] each result in a 0.2 fs uncertainty in the lifetime.

Consistency of the results is tested by repeating the full analysis in subsets of the data split according to data-taking periods and conditions, $\Omega_c^0$ momentum and flight direction, charm flavor, and $\Omega^-$ flight length. In all cases, the variations of the results are consistent with statistical fluctuations. To check that the best-candidate selection in events with multiple candidates does not affect the result, the measurement is repeated with randomly selecting a single candidate, removing all events with multiple candidates, or keeping all candidates. No significant variation in the measured lifetime is observed. The measurement is also repeated with the fit range varied to exclude candidates in the tails of the $(t, \sigma_t)$ distribution, with no significant deviation in the resulting lifetime from the nominal result.

In conclusion, we report on a measurement of the $\Omega_c^0$ lifetime using $e^+e^- \to c\overline{c}$ data collected by the Belle II experiment corresponding to an integrated luminosity of $207\,\text{fb}^{-1}$. This measurement,

$$\tau(\Omega_c^0) = 243 \pm 48\,(\text{stat}) \pm 11\,(\text{syst})\,\text{fs}\,,$$

is consistent with the LHCb average of $274.5 \pm 12.4$ fs [14], and inconsistent at 3.4 standard deviations with the pre-LHCb world average of $69 \pm 12$ fs [10]. The Belle II result, therefore, confirms that the $\Omega_c^0$ is not the shortest-lived weakly decaying charmed baryon.

### Acknowledgments

We thank the SuperKEKB group for the excellent operation of the accelerator; the KEK cryogenics group for the efficient operation of the solenoid and the KEK computer group for on-site computing support.

[1] M. Neubert, *B decays and the heavy quark expansion*, Adv. Ser. Direct. High Energy Phys. **15** (1998) 239, arXiv:hep-ph/9702375.

[2] N. Uraltsev, *Topics in the heavy quark expansion*, in *At the frontier of Particle Physics*, M. Shifman and B. Ioffe, eds. 2001. arXiv:hep-ph/0010328.

[3] A. Lenz and T. Rauh, *D-meson lifetimes within the heavy quark expansion*, Phys. Rev. D **88** (2013) 034004, arXiv:1305.3588 [hep-ph].

[4] A. Lenz, *Lifetimes and heavy quark expansion*, Int. J. Mod. Phys. A **30** (2015) 1543005, arXiv:1405.3601 [hep-ph].

[5] M. Kirk, A. Lenz, and T. Rauh, *Dimension-six matrix elements for meson mixing and lifetimes from sum rules*, JHEP **12** (2017) 068, arXiv:1711.02100 [hep-ph]. Erratum JHEP **06** (2020) 162.

[6] H.-Y. Cheng, *Phenomenological study of heavy hadron lifetimes*, JHEP **11** (2018) 014, arXiv:1807.00916 [hep-ph].

[7] P. A. Zyla et al., Particle Data Group, *Review of Particle Physics*, PTEP **2020** (2020) 083C01.

[8] P. L. Frabetti et al., E687 collaboration, *First measurement of the lifetime of the $\Omega_c^0$*, Phys. Lett. B **357** (1995) 678.

[9] M. I. Adamivich et al., WA89 collaboration, *Measurement of the $\Omega_c^0$ lifetime*, Phys. Lett. B **358** (1995) 151, arXiv:hep-ex/9507004.

[10] M. Tanabashi et al., Particle Data Group, *Review of Particle Physics*, Phys. Rev. D **98** (2018) 030001.

[11] M. A. Shifman and M. B. Voloshin, *Hierarchy of Lifetimes of Charmed and Beautiful Hadrons*, Sov. Phys. JETP **64** (1986) 698.

[12] B. Guberina, R. Ruckl, and J. Trampetic, *Charmed Baryon Lifetime Differences*, Z. Phys. C **33** (1986) 297.

[13] R. Aaij et al., LHCb collaboration, *Measurement of the $\Omega_c^0$ baryon lifetime*, Phys. Rev. Lett. **121** (2018) 092003, arXiv:1807.02024 [hep-ex].

[14] R. Aaij et al., LHCb collaboration, *Measurement of the lifetimes of promptly produced $\Omega_c^0$ and $\Xi_c^0$ baryons*, Sci. Bull. **67** (2022) no. 5, 479–487, arXiv:2109.01334 [hep-ex].

[15] H.-Y. Cheng, *The strangest lifetime: A bizarre story of $\tau(\Omega_c^0)$*, Sci. Bull. **67** (2022) no. 5, 445–447, arXiv:2111.09566 [hep-ph].

[16] J. Gratrex, B. Melić, and I. Nišandžić, *Lifetimes of singly charmed hadrons*, arXiv:2204.11935 [hep-ph].

[17] T. Abe, Belle II collaboration, *Belle II Technical Design Report*, arXiv:1011.0352 [physics.ins-det].

[18] K. Akai, K. Furukawa, and H. Koiso, *SuperKEKB Collider*, Nucl. Instrum. Meth. **A907** (2018) 188, arXiv:1809.01958 [physics.acc-ph].

[19] T. Kuhr, C. Pulvermacher, M. Ritter, T. Hauth, and N. Braun, Belle II framework software group, *The Belle II Core Software*, Comput. Softw. Big Sci. **3** (2019) 1, arXiv:1809.04299 [physics.comp-ph].

[20] The Belle II Collaboration, *Belle II Analysis Software Framework (basf2)*, https://doi.org/10.5281/zenodo.5574115.

[21] S. Jadach, B. F. L. Ward, and Z. Wąs, *The precision Monte Carlo event generator KK for two-fermion final states in $e^+e^-$ collisions*, Comput. Phys. Commun. **130** (2000) 260, arXiv:hep-ph/9912214 [hep-ph].

[22] T. Sjöstrand, S. Ask, J. R. Christiansen, R. Corke, N. Desai, P. Ilten, S. Mrenna, S. Prestel, C. O. Rasmussen, and P. Z. Skands, *An Introduction to*

*PYTHIA 8.2*,
Comput. Phys. Commun. **191** (2015) 159,
arXiv:1410.3012 [hep-ph].

[23] D. J. Lange, *The EvtGen particle decay simulation package*, Nucl. Instrum. Meth. **A462** (2001) 152.

[24] S. Agostinelli et al., GEANT4 collaboration, *GEANT4: A Simulation toolkit*,
Nucl.Instrum.Meth. **A506** (2003) 250.

[25] J.-F. Krohn et al., Belle II analysis software group, *Global decay chain vertex fitting at Belle II*,
Nucl. Instrum. Meth. **A976** (2020) 164269,
arXiv:1901.11198 [hep-ex].